Free Radical Research, April 2011; 45(4): 483–495

Schisandrin B elicits a glutathione antioxidant response and protects against apoptosis via the redox-sensitive ERK/Nrf2 pathway in AML12 hepatocytes

POU KUAN LEONG, PO YEE CHIU, NA CHEN, HOI YAN LEUNG & KAM MING KO

Section of Biochemistry and Cell Biology, Division of Life Science, The Hong Kong University of Science & Technology, Clear Water Bay, Hong Kong SAR, PR China

(Received date: 3 November 2010; Accepted date: 22 December 2010)

Abstract

This study examined the effects of (–)schisandrin B [(–)Sch B] on MAPK and Nrf2 activation and the subsequent induction of glutathione antioxidant response and cytoprotection against apoptosis in AML12 hepatocytes. Pharmacological tools, such as cytochrome P-450 (CYP) inhibitor, antioxidant, MAPK inhibitors and Nrf2 RNAi, were used to delineate the signalling pathway. (–)Sch B caused a time-dependent activation of MAPK in AML12 cells, particularly the ERK1/2. The MAPK activation was followed by an enhancement in Nrf2 nuclear translocation and the eliciting of a glutathione antioxidant response. Reactive oxygen species arising from a CYP-catalysed reaction with (–)Sch B seemed to be causally related to the activation of MAPK and Nrf2. ERK inhibition by U0126 or Nrf2 suppression by Nrf2 RNAi transfection almost completely abrogated the cytoprotection against menadione-induced apoptosis in (–)Sch B-pre-treated cells. (–)Sch B pre-treatment potentiated the menadione-induced ERK activation, whereas both p38 and JNK activations were suppressed. Under the condition of ERK inhibition, Sch B treatment did not protect against carbon tetrachloride-hepatotoxicity in an *in vivo* mouse model. In conclusion, (–)Sch B triggers a redox-sensitive ERK/Nrf2 signalling, which then elicits a cellular glutathione antioxidant response and protects against oxidant-induced apoptosis in AML12 cells.

Keywords: *Schisandra chinensis, reactive oxygen species, liver, redox signalling, menadione*

Abbreviations: *ABT, 1-amino-benzotriazole; AIF, apoptosis inducing factor; CYP, cytochrome P-450; DTT, dithiothreitol; EpRE, electrophile response element; ERK, extracellular signal-regulated protein kinase; GCL, γ-glutamyl cysteine ligase; G6PDH, glucose-6-phosphate dehydrogenase; GR, glutathione reductase; GSH, reduced glutathione; JNK, C-jun-NH_2-terminal kinases; SDH, sorbitol dehydrogenase; MAPK, mitogen-activated protein kinases; mGCL, modulatory sub-unit of GCL; Nrf2, nuclear factor erythroid 2-related factor 2; p38, p38 MAPK; PMSF, phenylmethylsulphonyl fluoride; ROS, reactive oxygen species; Sch B, schisandrin B.*

Introduction

Schisandrin B (Sch B) is the most abundant and active dibenzocyclooctadiene derivative isolated from the fruit of *Schisandra chinensis* (Fructus Schisandrae), a commonly used Chinese herb for promoting health and which is also clinically prescribed for the treatment of viral and chemical hepatitis [1]. An early study in our laboratory has demonstrated that Sch B protected against carbon tetrachloride (CCl_4) hepatotoxicity in mice [2]. The hepatoprotection afforded by Sch B pre-treatment was found to be associated with the enhancement in mitochondrial glutathione antioxidant system and heat shock protein expression [3]. Recent studies have suggested that reactive oxidant species (ROS) generated from cytochrome P-450 (CYP), or CYP2E1 in particular, catalysed metabolism of Sch B may trigger the antioxidant and heat shock responses in mouse liver [4,5]. The hepatoprotection afforded by Sch B seemed to be mechanistically related to the increased resistance of mitochondria to Ca^{2+}-induced

Correspondence: Dr Kam Ming Ko, Section of Biochemistry and Cell Biology, Division of Life Science, The Hong Kong University of Science and Technology, Clear Water Bay, Hong Kong SAR, PR China. Tel: 852 2358 7298. Fax: 852 2358 1552. Email: bcrko@ust.hk

ISSN 1071-5762 print/ISSN 1029-2470 online © 2011 Informa UK, Ltd.
DOI: 10.3109/10715762.2010.550917

permeability transition [6]. In cultured AML12 hepatocytes, a cell line derived from mouse liver, Sch B treatment could enhance cellular glutathione level and protect against oxidant injury [7]. The Sch B preparation used in earlier investigations was found to be a mixture of (±) γ-schisandrin and (−)Sch B (or gomisin N)—(−)Sch B having been found to be more prominent than (±) γ-schisandrin in protecting against menadione toxicity [8] and hypoxia/reoxygenation-induced apoptosis in AML12 cells [9]. Parallel with observations in animal studies, the cytoprotection against hypoxia/reoxygenation-induced apoptosis afforded by (−)Sch B pre-treatment was accompanied by an increase in mitochondrial membrane potential and a decrease in the extent of Ca^{2+}-induced mitochondrial permeability transition [9].

Previous studies have suggested that Sch B-induced cellular glutathione antioxidant and heat shock responses are causally related to the hepatoprotective effect against CCl_4-hepatotoxicity [3]. Nevertheless, the biochemical mechanism underlying the Sch B-induced cytoprotective effects has not been investigated yet. Given that methylenedioxy group-containing compounds were found to be metabolized by the cytochrome P-450 (CYP) system [10], Sch B is also expected to be a substrate for CYP and thereby produces reactive oxygen species (ROS) through CYP-catalysed biotransformation. In this connection, our recent study showed that CYP-mediated metabolism of Sch B was associated with increased ROS production in mouse liver microsomes and that the Sch B-induced glutathione antioxidant response and hepatoprotection were suppressed by antioxidant pre-treatment in mice (unpublished data). This observation was corroborated by results obtained from studies which demonstrated the ability of (−)Sch B to stimulate the glutathione antioxidant response in a CYP- and ROS-dependent manner in AML12 cells [11].

ROS not only serve as deleterious species in the cellular system, but also are important intracellular redox signalling molecules [12]. The dual function of ROS in regulating cell survival and death suggests their role in redox signalling wherein mitogen-activated protein kinases (MAPK) play an essential role [13,14]. The stimulation of adaptive responses to oxidative stress requires one or more members of the MAPK cascade. The ultimate effects of MAPK activation depend on their ability to phosphorylate the downstream signalling molecules, subsequently express appropriate genes and thereby manifest a cellular redox homeostasis. Among the three distinct MAPK pathways, extracellular signal-regulated protein kinase (ERK) is activated by mitogens and growth factors [15], whereas C-Jun-NH2-terminal kinases (JNK) and p38 MAPK (p38) are regulated by extracellular stresses such as UV, ionizing radiation and oxidative stress [16,17]. Upon their activation, ERK, JNK and p38 can phosphorylate a range of transcription factors [13], which in turn change the profiles of gene expression that result in biological responses [18,19].

Nuclear factor erythroid 2-related factor 2 (Nrf2) is a redox-sensitive transcription factor that binds the electrophile response element (EpRE). It has been shown that translocation of Nrf2 from the cytosol to the nucleus is facilitated by phosphorylation [20,21], with subsequent enhancement in the expression of antioxidant defence genes [22]. In essence, the nuclear Nrf2 binds on specific sequences of EpRE within the promoter region of target genes encoding many stress-responsive or cytoprotective enzymes/proteins, including the subunits of γ-glutamyl cysteine ligase (GCL), glutathione S-transferases and NAD(P)H-quinone oxidoreductase, etc. [23,24].

Here, we hypothesize that through the CYP-mediated biotransformation, (−)Sch B can elicit a glutathione antioxidant response via a MAPK signalling pathway in AML12 cells (Figure 1). In the present study, we therefore investigated the redox signalling triggered by (−)Sch B by examining the MAPK/Nrf2 signalling pathway. To confirm the finding in a cell model system, the role of the ERK signalling pathway in Sch B-induced hepato-protection was examined in an *in vivo* mouse model of hepatotoxicity using a specific ERK inhibitor U0126.

Methods

Preparation of (–)Sch B

Sch B (consisting of a mixture of Sch B stereoisomers) was prepared from the petroleum extract of Fructus Schisandrae using silica gel chromatography, as described by Ip et al. [2]. (–)Sch B was then isolated from Sch B by preparative HPLC, as described in Chiu et al. [8,9].

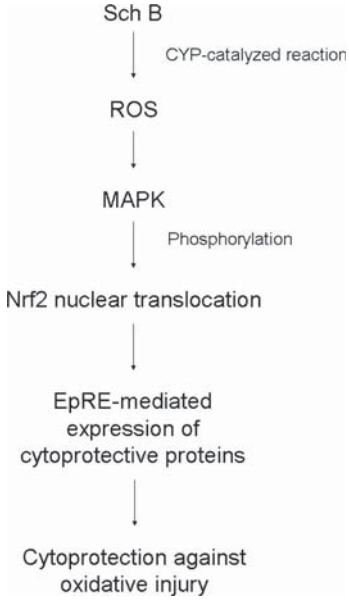

Figure 1. Postulated signalling pathway induced by (–)Sch B.

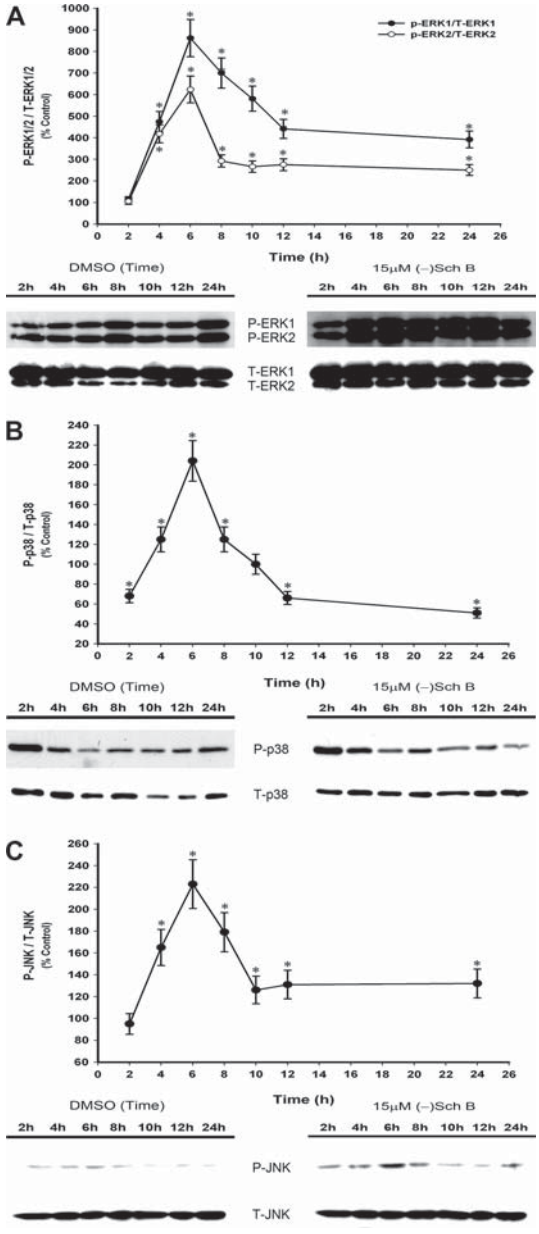

Figure 2. Time course of (–)Sch B-induced MAPK activation in AML12 cells. Cells were treated with (–)Sch B at 15 μM. The ratio of phospho-kinase level to total kinase level for (A) ERK1/2, (B) p38 and (C) JNK were expressed as % control (with respect to the time-matched DMSO control). Values given are means ± SD, with data obtained from triplicate samples in the same experiment. *Significantly different from the time-matched DMSO control.

Cell culture

AML12 hepatocytes were cultured as monolayers using Dulbecco's modified Eagle's medium/F12 (GIBCO BRL) supplemented with 10% foetal bovine serum, 100 units/mL penicillin, 0.1 mg/mL streptomycin, 40 ng/mL dexamethasone and ITS (containing 5 mg/L insulin, 5 mg/L transferrin and 5 μg/L selenium). Cells were grown in 75 cm^2 flasks and kept at 37°C in a humidified atmosphere of air (i.e. ~ 21% O_2) and 5% CO_2. Cells were grown at 80% of confluence prior to the exposure to drugs in the various experiments.

Western blot analysis of MAPK

Cells were incubated with 15 μM (–)Sch B or vehicle (i.e. DMSO, 0.2% (w/w) final concentration) for increasing periods of time (2–24 h). Cells for ERK1/2 analysis were first incubated with serum-free medium for a 24-h period of starvation, which was followed by incubation with drug-containing serum-free medium. Cells for p38 and JNK analyses were incubated with drug-containing normal medium. After incubating with (–)Sch B, cells were lysed with 500 μL of lysis buffer (20 mM Tris-HCl, 2 mM EDTA, 3 mM EGTA, 1% Triton X-100, 10% glycerol, 5% SDS, 1 mM dithiothreitol (DTT), 5 μg/mL leupeptin, 5 μg/mL aproptinin, 5 μg/mL pepstain, 1 μM phenylmethylsulphonyl fluoride (PMSF), pH 7.5). The lysates were further processed by repetitively passing through a 30G 1/2 syringe needle (10 times) and protein concentrations in cell lysates were determined by using a DC Protein Assay kit (Bio-Rad Laboratories, Hercules, CA). Equal amounts of total cell lysate (10–40 μg of protein) were subjected to 12% SDS-PAGE, followed by overnight Western blotting of phosphorylated MAPK using rabbit polyclonal antibodies specific for phospho-p44/42 MAPK (ERK1/2), phospho-p38 or phospho-JNK, respectively. The total MAPK levels were analysed by stripping the membranes with stripping buffer (Pierce, Rockfork, IL) at 37°C for 30 min, and the membranes were then re-probed using anti-p44/p42 MAPK (ERK1/2) antibody, anti-p38 antibody or anti-JNK antibody, respectively. Then, after the incubation with second antibodies (1:2000; Cell Signaling Technology, Beverly, MA), immuno-stained bands were quantitatively analysed by densitometry using an ECL Western Blot System (Cell Signaling Technology). All MAPK antibodies were purchased from Cell Signaling Technology and were used at a dilution of 1:1000. The extent of (–)Sch B-induced MAPK activation was estimated by computing the ratio of phosphorylated-MAPK to total-MAPK level in (–)Sch B-treated cells with respect to the time-matched DMSO control.

Cellular GSH level and Western blot analysis of glutathione-related antioxidant proteins

Cells were firstly treated with 15 μM (–)Sch B for 6 h, followed by the incubation with fresh medium (without drug) for increasing periods of time (4–18 h). Cell lysates were prepared at the indicated period of time. For the measurement of cellular GSH levels, the reduced glutathione (GSH) level in cell lysates was

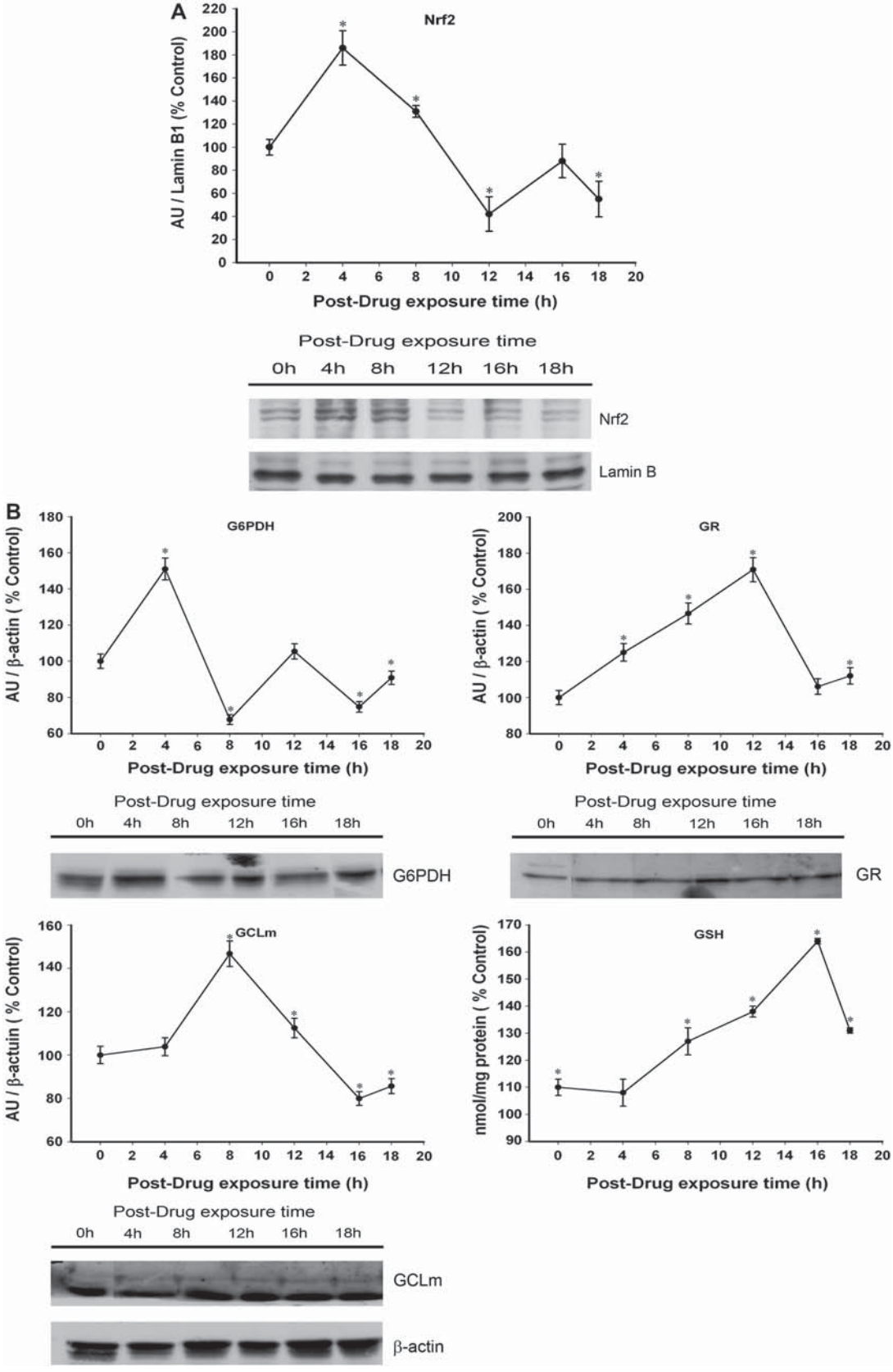

Figure 3. Post-drug exposure time course of (–)Sch B-induced Nrf2 activation and glutathione antioxidant response in AML12 cells. Cells were treated with (–)Sch B for 6 h and then followed by incubation with the culture medium without drug. Levels of (A) Nrf2, (B) reduced gltuathione (GSH, Levels of (A) Nrf2, (B) reduced gltuathione (GSH), γ-glutamyl cysteine ligase modulatory sub-unit (GCLm), glutathione reductase (GR) and glucose-6-phosphate dehydrogenase (G6DPH) were measured and expressed in % control (with respect to the value immediately after post-(–)Sch B exposure (i.e. time 0)). Values given are means ± SD, with data obtained from triplicate samples in the same experiment. *Significantly different from the respective value at time 0.

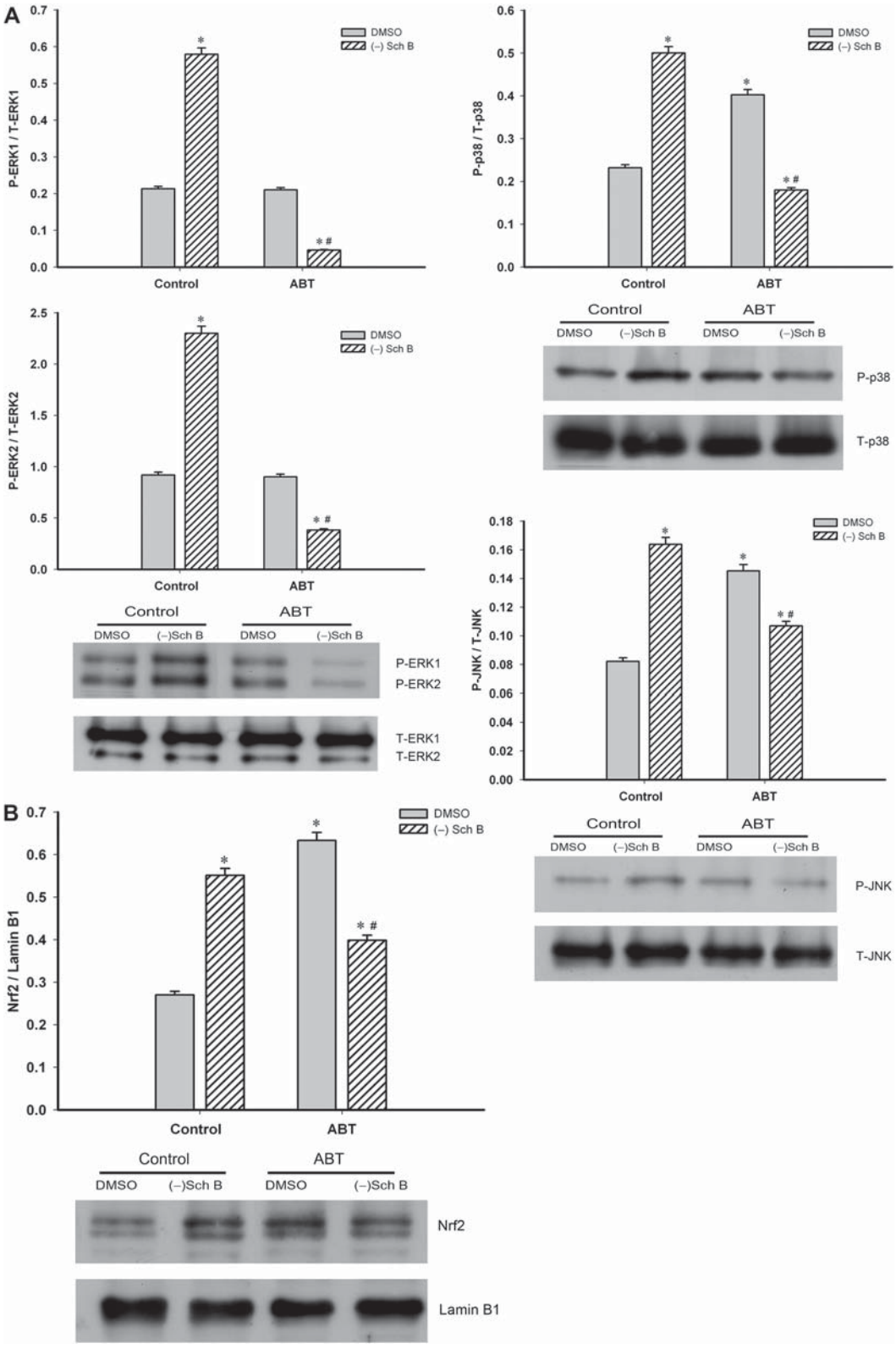

Figure 4. Effects of ABT on (–)Sch B-induced MAPK and Nrf2 activation. Cells were pre- and co-treated with 1-aminobenzotriazole (ABT, 10 mM) prior to and during the incubation with (–)Sch B at 15 μM for 6 h. The extent of MAPK activation was assessed by the measurement of the ratio of phospho-kinase level to total kinase level (A). Nuclear Nrf2 levels were measured (B). Values given are means ± SD, with data obtained from triplicate samples in the same experiment. *Significantly different from the DMSO control group; #significantly different from the DMSO with the ABT group.

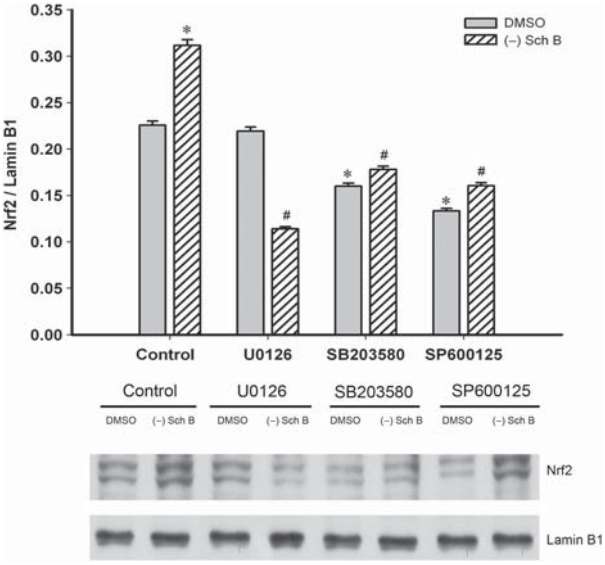

Figure 5. Effects of MAPK inhibitors on (–)Sch B-induced Nrf2 activation. Cells were treated with (–)Sch B (15 μM) for 6 h without or with specific inhibitor of ERK1/2 (U0126, 10 μM), p38 (SB203580, 10 μM) or JNK (SP600125, 10 μM). Nuclear Nrf2 levels were measured. Values given are mean ± SD, with data obtained from triplicate samples in the same experiment. *Significantly different from the DMSO control group; #significantly different from the DMSO with the respective MAPK inhibitor group.

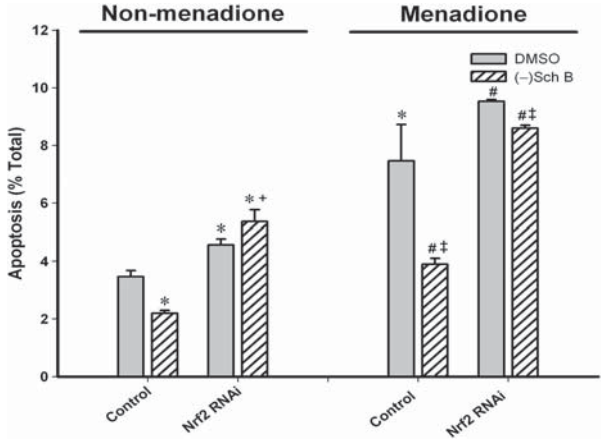

Figure 7. Effect of Nrf2 RNAi on (–)Sch B-induced protection against apoptosis in AML12 cells. Cells were transfected with Nrf2 RNAi, as described in Materials and methods, and exposed to (–)Sch B (15 μM) for 6 h. Sixteen hours after (–)Sch B exposure, cells were subjected to menadione challenge, as described in Figure 6. Values given are means ± SD, with data obtained from triplicate samples in the same experiment. *Significantly different from the non-menadione DMSO control group; †significantly different from the non-menadione DMSO control with Nrf2 RNAi; #significantly different from the menadione DMSO group; ‡significantly different from the menadione DMSO control with Nrf2 RNAi.

measured using an enzymatic method of Griffith [25]. For measurements of glutathione-related antioxidant proteins, equal amounts of total cell lysates (50 μg protein) were subjected to 10–15% SDS-PAGE, followed by Western blotting using antibodies against each of the various glutathione-related antioxidant proteins. All antibodies were rabbit polyclonal antibodies, which are specific for the modulatory sub-unit of GCL (GCLm) (1:500; Santa Cruz Biotechnology, Santa Cruz, CA), for GR (1:500; Santa Cruz Biotechnology) and for glucose-6-phosphate dehydrogenase (G6PDH) (1:500, Abcam, Cambridge, CA). All immunostained bands were analysed by densitometry and the amounts (arbitrary units) of various proteins were normalized with reference to β-actin (1:1000 antibodies, Cell Signaling Technology) levels (arbitrary units) in the sample.

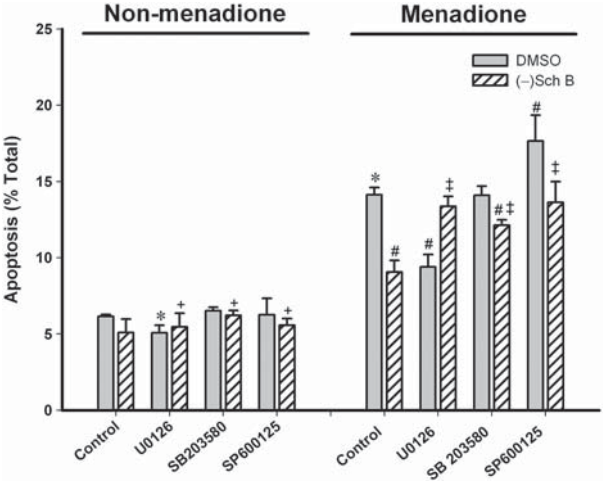

Figure 6. Effects of MAPK inhibitors on (–)Sch B-induced protection against apoptosis in AML12 cells. Cells were treated with (–)Sch B without or with specific MAPK inhibitors for 6 h, as described in Figure 5. Sixteen hours after drug exposure, cells were subjected to 1 h of menadione (20 μM) challenge. The extent of apoptotic cell death was measured by flow cytometry. Values given are mean ± SD, with data obtained from triplicate samples in the same experiment. *Significantly different from the non-menadione DMSO control group; †significantly different from the non-menadione DMSO group with the respective MAPK inhibitor; #significantly different from the menadione DMSO control group; ‡significantly different from the menadione DMSO control group with the respective MAPK inhibitor.

Preparation of nuclear extracts and Western blot analysis of Nrf2

Cells were treated with (–)Sch B as described above. Cells were harvested by trypsinization and the nuclear fraction prepared as described in Cullinan et al. [26]. The nuclear fractions were mixed with six volumes of SDS buffer (1 M Tris-HCl, pH 6.8, 10% SDS, 30% glycerol, 6 mM DTT and 0.2 mM bromophenol blue) and the nuclear protein concentrations were determined using a DC Protein Assay kit. Equal amounts of nuclear proteins (40 μg) were subjected to 10% SDS-PAGE and Western blot analysis using Nrf2 antibodies (1:500; Santa Cruz Biotechnology) was performed as described above. The amounts (arbitrary units) of Nrf2 were normalized with reference to lamin B1 (1:3000 antibodies, Abcam) levels (arbitrary units) in the sample.

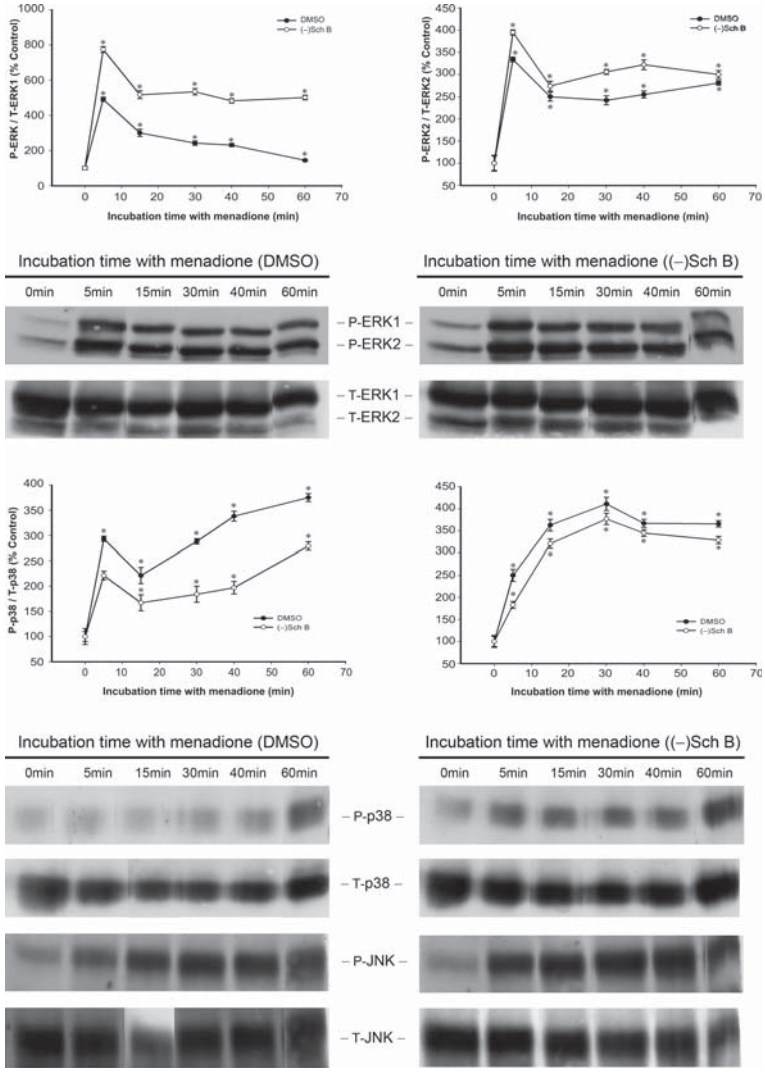

Figure 8. Effects of (–)Sch B pre-treatment on menadione-induced changes in MAPK activation. Cells were treated with (–)Sch B (15 μM) for 6 h and then incubated with culture medium for 16 h. Then, the cells were subjected to 1 h of menadione challenge. Phosphorylation of ERK1/2, p38 and JNK were measured as described in Figure 2. Values given are means ± SD, with data obtained from triplicate samples in the same experiment. *Significantly different from the respective value at time 0.

Effect of a CYP450 inhibitor on MAPK and Nrf2 activation

Cells were pre-incubated with 1-aminobenzotriazole (ABT) (10 mM final concentration, 2 h) prior to the addition of 15 μM (−)Sch B. Cells were co-incubated with ABT and (−)Sch B for 6 h and then lysed with 500 μL of ice-cold SDS-containing lysis buffer. For the study on Nrf2 activation, cells were seeded (1×10^6 cells/100 mm plate) and cultured for 48 h. Cells were pre-incubated with ABT prior to (−)Sch B treatment and then co-incubated with ABT and (−)Sch B for 6 h, followed by fresh medium for 4 h. The cells were then harvested and nuclear fractions were obtained as described above. Equal amounts of nuclear proteins (40 μg) were subjected to 10% or 12% SDS-PAGE and Western blot analysis using Nrf2 antibodies or different MAPK antibodies were performed.

Effect of MAPK inhibition on Nrf2 activation

The ERK inhibitor (U0126, 10 μM for 1 h, Cell Signaling Technology), p38 inhibitor (SB203580, 10 μM for 30 min, Sigma, St. Louis, MO) or JNK inhibitor (SP600125, 10 μM for 30 min, Sigma) was added prior to the addition of (−)Sch B to the AML12 cells. Cells were then co-incubated with the respective MAPK inhibitor and 15 μM (−)Sch B for 6 h, followed by the addition of fresh medium for an additional 4 h. The nuclear fractions of the cells were prepared and Nrf2 levels were analysed by Western blot analysis as described above.

Effect of MAPK inhibition on cytoprotection against apoptosis

Cells were treated with the respective MAPK inhibitor prior to the addition of (−)Sch B in AML12 cells,

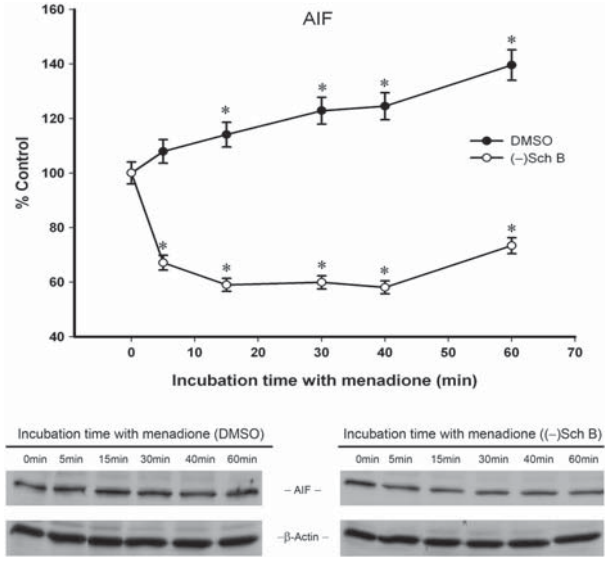

Figure 9. Effect of (–)Sch B pre-treatment on menadione-induced change in AIF release in AML12 cells. Cells were treated with (–)Sch B and then subjected to menadione challenge, as described in Figure 8. Cytosolic apoptosis-inducing factor (AIF) levels were measured. Values given are means ± SD, with data obtained from triplicate samples in the same experiment. *Significantly different from the respective value at time 0.

as described above. Cells were then co-incubated with MAPK inhibitor and 15 μM Sch B for 6 h, followed by incubation with fresh medium for an additional 16 h. Immediately following the treatment, the cells were challenged with menadione (20 μM, 0.2% (v/v) ethanol final concentration in a FBS-free medium for ERK and in a complete medium with FBS for JNK and p38) for 1 h. The extent of apoptotic cell death was measured by flow cytometry (COULTER®EPICS®XLTM, Beckman Coulter, Fullerton, CA) using Annexin V-FITC-Fluos (Roche, Penzberg, Germany) using propidium iodide (Sigma) for staining. Total apoptotic cell death was calculated by summing the percentages of cells in early apoptosis and late apoptosis.

Knockdown Nrf2 expression by siRNA

Transfection with Nrf2 siRNA was performed according to the manufacturer's instructions using the target sequence of sense, 5-UUAAGUGGCCCAAGUC UUGCUCCA-3; anti-sense, 5-UGGAGCAAGACU UGGGCCACUUAAA-3 for Nrf2 siRNA (Invitrogen, Eugene, OR). Cells were transfected with Nrf2 siRNA (50 nmol/L) with Lipofectamin RNAiMAX transfection reagent (Invitrogen) according to the procedures modified from Erfle et al. [27]. The transfection efficiency of siRNA, as assessed by using BLCOK-iTTM Fluorescent Oligo (Invitrogen), was found to be 95%. The degree of Nrf2 knockdown 24 h after transfection was determined by Western blot analysis, using an anti-Nrf2 antibody. Immuno-stained bands were quantified as described above.

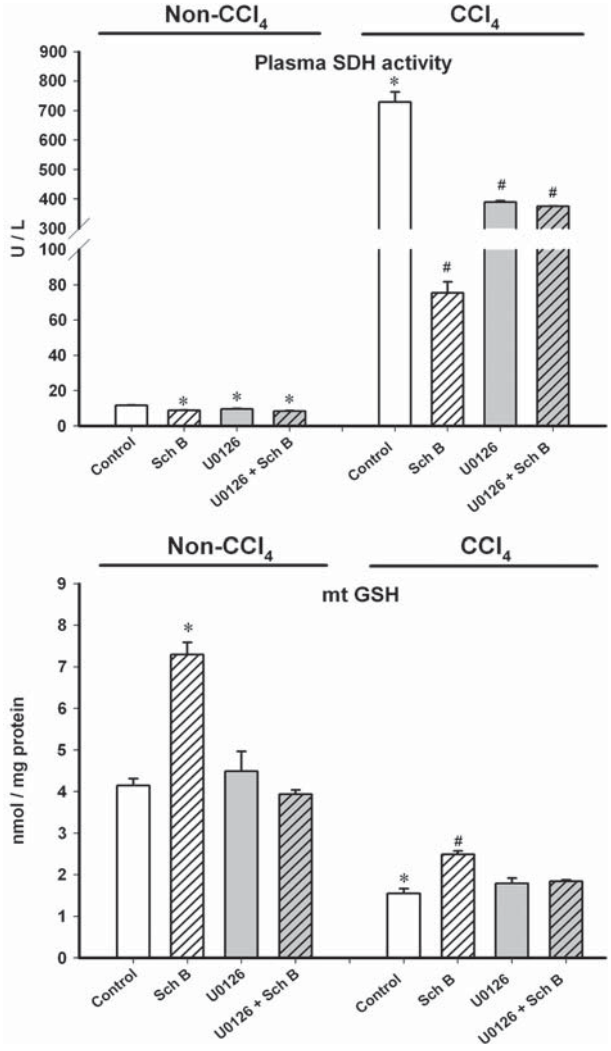

Figure 10. Effect of ERK inhibition on Sch B-induced protection against carbon tetrachloride hepatotoxicity in mouse liver *in vivo*. Mice were intraperitoneally injected with U0126 (5 mg/kg) prior to the oral administration of Sch B at 2 mmol/kg. Twenty-four hours after the drug treatment, Sch B-pre-treated mice were orally administrated with carbon tetrachloride (CCl_4) (0.1 ml/kg). Twenty-four hours post-challenge, the extent of CCl_4-induced injury was assessed by plasma sorbital dehydrogenase (SDH) activity. Hepatic mitochondrial GSH level was also measured. Values given are mean ± SEM, with $n = 5$. *Significantly different from the non-CCl_4 control; #significantly different from the CCl_4 control.

Effect of Nrf2 knockdown on cytoprotection against apoptosis

The Nrf2 siRNA transfected cells were then exposed to 15 μM (−)Sch B for 6 h, followed by incubation with fresh medium for 16 h. The cells were then challenged with menadione (20 μM) for 1 h and the extent of apoptosis was estimated by flow cytometry, as described above.

Time course of MAPK activation upon menadione-toxicity

The cells were pre-treated with (−)Sch B as described above. The cells were then challenged with menadione

(20 μM) for 1 h. Cells were lysed with 500 μL of SDS-containing lysis buffer at the indicated time points. Protein concentrations of the lysates were determined and equal amounts of protein were subjected to 12% SDS-PAGE and Western blot analysis was performed for MAPK, as described above.

Time course of change in apoptosis inducing factor (AIF) release upon menadione toxicity

Cells were treated with (−)Sch B and challenged with menadione (20 μM) for 1 h, as described above. Then cells were lysed with 500 μL of SDS-containing lysis buffer at the indicated time points. Equal amounts of proteins (40 μg) were subjected to 10% SDS-PAGE and Western blot analysis using anti-AIF (1:1000, Cell Signaling Technology) antibodies was performed. The amount of AIF released (arbitrary unit) was normalized with reference to the β-actin level (arbitrary unit) in the sample.

Effect of ERK inhibition on Sch B-induced protection against CCl_4-induced hepatotoxicity in vivo

Adult female Balb/c mice (8–10 weeks old, 20–25 g) were maintained under a 12-h dark/light cycle at ~ 22°C and allowed food and water *ad libitum* in the Animal and Plant Care Facility at the Hong Kong University of Science and Technology (HKUST). All experimental protocols were approved by the University Committee on Research Practice at HKUST.

Animals were randomly divided into groups of five animals. Mice were injected with ERK inhibitor (U0126, 5 mg/kg, i.p.) 1 h prior to the Sch B treatment. Sch B (dissolved/suspended in olive oil) was intragastrically administered at a single dose of 2 mmol/kg. ERK inhibitor or Sch B untreated animals were given the vehicle only. For the CCl_4-treated mice, 24 h after the Sch B treatment, mice were orally administered with 0.1 mL/kg CCl_4 (0.01%, v/v, in olive oil). Then, 24 h after CCl_4 challenge (all animals survived), heparinized blood samples and liver tissue samples were obtained. The extent of CCl_4-induced oxidative injury was assessed by plasma sorbital dehydrogenase (SDH) activity.

Hepatic tissue samples were rinsed with ice-cold isotonic buffer (210 mM mannitol, 70 mM sucrose, 5 mM HEPES, 1 mM EGTA, pH 7.4). Tissue homogenates were prepared by homogenizing 0.8 g of minced tissues in 8 mL ice-cold isotonic buffer. The homogenates were centrifuged at 600 × *g* for 20 min. After collecting the supernatants, the pellets were resuspended with the same volume of ice-cold isotonic buffer and re-centrifuged at 600 × *g* again. The procedure was repeated twice. The pooled supernatants were centrifuged at 8000 × *g* for 30 min and the mitochondrial pellets were collected. The mitochondrial pellets were resuspended in 0.5–1.0 mL of ice-cold isotonic buffer and constituted the mitochondrial fractions. Mitochondrial GSH level was measured as previously described [3].

Statistical analysis

Data were analysed by one-way Analysis of Variance. Post-hoc multiple comparisons were performed using Least Significant Difference test. *P*-values <0.05 were regarded as a statistically significant difference.

Results

(−)Sch B-induced a time-dependent MAPK activation

Figure 2 shows that (−)Sch B treatment (15 μM) caused time-dependent increases in the ratio of phospho-kinase to total kinase level of ERK1/2 (A), p38 (B) and JNK (C) in AML12 cells, implicating the activation of MAPK. Maximum extents of activation for all MAPK were observed at 6 h post (−)Sch B treatment, with the degree of ERK1/2 phosphorylation (862 and 624%) being larger than those of p38 (204%) and JNK (223%), when compared with the time-matched vehicle (i.e. DMSO) control.

(−)Sch B induced a time-dependent Nrf2 activation and subsequent glutathione antioxidant response after 6-h drug treatment

Six-hour exposure to (−)Sch B caused a time-dependent change in nuclear Nrf2 level, an indirect measure of Nrf2 activation, in AML12 cells, with the degree of stimulation being maximum (87%, compared to the value obtained immediately after drug exposure, i.e. time 0) at 4 h post-drug treatment (Figure 3A). Then the Nrf2 level decreased beyond the time 0 value at 12 h post-drug exposure and slightly increased thereafter. The increase in nuclear Nrf2 level was associated with simultaneous or later induction of the expression of enzymes related to glutathione redox cycling and synthesis, namely G6DPH, GR and GCLm, with the maximum degree of stimulation occurring at 4 h post-drug exposure for G6PDH (51%), 8 h post-drug exposure for GCLm (47%) and 12 h post-drug exposure for GR (47%) (Figure 3B). While GCLm and G6DPH levels declined from the peak to values beyond the time 0 levels at 18 h post-drug exposure, the decrease of GR level from the peak returned to time 0 level at 18 h post-drug exposure (Figure 3B). The 6-h drug treatment with (−)Sch B caused a time-dependent increase in cellular GSH level, with the extent of enhancement being maximum (64%) at 16 h post-drug treatment (Figure 3B). Then, their levels declined after reaching the peak.

(−)Sch B did not induce the activation of MAPK and Nrf2 in the presence of ABT

To define the role of CYP in (−)Sch B-induced signal transduction, we examined the effects of ABT (a broad-spectrum CYP inhibitor) on MAPK activation and nuclear Nrf2 level in (−)Sch B-treated AML12 cells. As shown in Figure 4A, while ABT (pre- and co-treatment) did not affect the phosphorylation of ERK1/2 in DMSO-treated (control) AML12 cells, (−)Sch B co-treatment decreased the phosphorylation of ERK1/2 at 6 h after the drug treatment. While ABT increased the phosphorylation of p38 and JNK in control cells, the phosphorylation of p38 and JNK were significantly suppressed by (−)Sch B co-treatment in ABT-treated cells. Figure 4B also shows that ABT increased the nuclear Nrf2 level in control AML12 cells, but (−)Sch B co-treatment decreased the nuclear Nrf2 level in ABT-treated cells at 4 h post-drug exposure.

(−)Sch B did not induce Nrf2 activation under ERK inhibition

Specific inhibitors of MAPK were used to investigate the causal relationship between (−)Sch B-induced MAPK activation and increase in nuclear Nrf2 levels in AML12 cells. Figure 5 shows that ERK inhibition did not cause any detectable changes in the nuclear Nrf2 level in AML12 cells, but (−)Sch B treatment decreased the nuclear Nrf2 level in the presence of ERK inhibition, with the level dropping below the control value at 4 h post-drug exposure. While p38 and JNK inhibition significantly decreased the nuclear Nrf2 level in control cells, (−)Sch B treatment induced a slight but significant increase in the nuclear Nrf2 level under the condition of p38 or JNK inhibition.

(−)Sch B did not protect against apoptosis under ERK inhibition

To further delineate the differential role of the three MAPK in the cytoprotection afforded by (−)Sch B, we investigated the effects of MAPK inhibitors on (−)Sch B-induced protection against apoptosis in AML12 cells. As shown in Figure 6, (−)Sch B treatment protected against menadione-induced apoptosis in AML12 cells. ERK inhibition decreased the extent of apoptosis in AML12 cells under menadione challenge, while JNK inhibition increased the extent of apoptosis. The inhibition of p38 did not affect the menadione-induced apoptosis. In the presence of ERK inhibitor, (−)Sch B treatment increased the extent of apoptosis under menadione-intoxication. However, under the condition of p38/JNK inhibition, (−)Sch B treatment still slightly but significantly decreased the extent of apoptosis in menadione-intoxicated cells.

Nrf2 RNAi transfection largely inhibited the (−)Sch B-induced protection against apoptosis

To define the critical role of Nrf2 in the cytoprotection afforded by (−)Sch B, we examined the effect of Nrf2 RNAi transfection on (−)Sch B-induced protection against apoptosis in AML12 cells. Figure 7 shows that (−)Sch B treatment protected against menadione-induced apoptosis in AML12 cells. Transfection of Nrf2 RNAi increased the extent of apoptosis in AML12 cells under control condition and (−)Sch B treatment slightly increased the extent of apoptosis in Nrf2 RNAi-transfected cells. In the menadione-intoxicated cells, the extent of apoptosis was dramatically increased in Nrf2 knockdown cells. (−)Sch B treatment protected against the apoptosis, but to a much lesser extent than that in non-Nrf2 RNAi transfected cells.

(−)Sch B pretreatment modulated the menadione-induced changes in MAPK activation

To further investigate the role of MAPK in the cytoprotection afforded by (−)Sch B against menadione-induced apoptosis, we examined the effect of (−)Sch B pre-treatment on menadione-induced MAPK activation in AML12 cells. As shown in Figure 8, menadione caused a time-dependent activation of MAPK AML12 cells, with the extent of stimulation of ERK1/2, p38 or JNK being maximum at 5 min, 60 min or 30 min, respectively. (−)Sch B enhanced the menadione-induced activation of ERK1/2, but suppressed those of p38 and JNK.

(−)Sch B pre-treatment suppressed the menadione-induced increase in AIF release

We also investigated the effects of (−)Sch B pre-treatment on menadione-induced change in AIF release in AML12 cells. Figure 9 shows that menadione intoxication caused a time-dependent AIF release in AML12 cells, with the extent of release being maximum at 60 min post-treatment. (−)Sch B pre-treatment significantly suppressed the menadione-induced AIF release up to 60 min post-challenge.

ERK inhibition abrogated the Sch B-induced hepatoprotection against CCl_4 toxicity in mice

To confirm the role of ERK activation in Sch B-induced hepatoprotection against CCl_4 toxicity *in vivo*, we examined the effect of ERK inhibition on CCl_4 hepatotoxicity and the associated change in mitochondrial GSH level in the liver of Sch B-pre-treated mice. Figure 10 shows that Sch B pre-treatment protected against CCl_4 hepatotoxicity, as evidenced by the significant decrease in the extent of plasma SDH activity. The hepatoprotection was associated with an increase in hepatic mitochondrial GSH level in non-CCl_4- or

CCl_4-treated mice. ERK inhibition did not affect the hepatic SDH leakage or mitochondrial GSH level in non-CCl_4-treated mouse livers and the hepatic SDH leakage or mitochondrial GSH level was not affected by Sch B pre-treatment under the condition of ERK inhibition. While the extent of CCl_4-induced SDH leakage was significantly reduced by ERK inhibition, (−)Sch B pre-treatment did not produce any detectable change in the SDH leakage under the condition of ERK inhibition. ERK inhibition did not produce any detectable changes in mitochondrial GSH level in livers isolated from CCl_4-treated mice, but Sch B pre-treatment slightly increased the mitochondrial GSH level under the condition of ERK inhibition.

Discussion

Recent studies from our laboratory have shown that the hepatoprotection against CCl_4 toxicity afforded by Sch B is causally related to the pro-oxidant effect of Sch B, presumably resulting from the CYP-catalysed metabolism of Sch B [4,5]. Studies using AML12 hepatocytes showed that (−)Sch B treatment induced the production of ROS in a CYP-dependent manner, which was followed by the eliciting of a glutathione antioxidant response [11]. In the present study, using the same drug treatment protocol, (−)Sch B was found to cause a time-dependent activation of MAPK. It is unlikely that the biological action produced by (−)Sch B is dependent on DMSO (drug vehicle) because a nanoemulsion of Sch B was also found to produce cytoprotective action in cell-based assay systems (unpublished data). MAPK play an important role in the regulation of cell survival and death [28,29]. Among the various MAPK signalling pathways, ERK signalling is commonly involved in upregulating cellular protective mechanism in response to xenobiotics in cultured mammalian cells [30,31]. In this connection, (−)Sch B was found to cause a much larger extent of activation of ERK as compared with that of p38 or JNK in AML12 cells. Given the role of ROS in activating the ERK signalling pathway [32,33], it is likely that the ROS arising from CYP-catalysed metabolism of (−)Sch B may also activate ERK. To test this postulation, interventional experiments were conducted to examine the role of CYP in (−)Sch B-induced activation of MAPK and Nrf2. While the activation of p38 and JNK as well as Nrf2 by ABT might be related to its CYP-mediated pro-oxidant activity, the ability of ABT to abrogate the (−)Sch B-induced ERK and Nrf2 activation supports the involvement of a CYP-catalysed reaction in the activation process. Nrf2, a redox sensitive transcription factor, is responsible for EpRE-driven expression of genes encoding the majority of antioxidant enzymes/proteins and phase II drug metabolizing enzymes [34]. It has been shown that Nrf2 is phosphorylated by ERK1/2 or JNK under conditions of oxidative stress, with a resultant nuclear translocation and the subsequent enhancement in the expression of antioxidant genes [35,36]. Taken together, our findings therefore suggest the involvement of a redox-sensitive MAPK/Nrf2 signalling pathway in eliciting the (−)Sch B-induced cellular glutathione antioxidant response and the associated protection against oxidant-induced cell apoptosis. This notion is supported by the finding that the knockdown of Nrf2 expression by Nrf2 RNAi transfection inhibited the cytoprotection against apoptosis in (−)Sch B-treated cells. In an attempt to clearly delineate the signal transduction pathway triggered by (−)Sch B, specific MAPK inhibitors were used to confirm their role in cytoprotective effect. The results indicated that ERK1/2 might be involved in the (−)Sch B-induced Nrf2 activation. The observation that (−)Sch B suppressed the basal Nrf2 activation in the presence of U0126 might reflect a decrease in cellular oxidative stress. The critical role of ERK1/2 was then supported by the finding that the inhibition of ERK, but not of p38 or JNK, completely abrogated the cytoprotection afforded by (−)Sch B against menadione-induced apoptosis in AML12 cells. The ability of U0126 to suppress the menadione-induced apoptosis might be due to the activation of a protective response in the presence of ERK inhibition in (−)Sch B-untreated cells.

The (−)Sch B-induced glutathione antioxidant response is characterized by increases in the expression of GCLm, GR and G6DPH, as well as an elevation of cellular GSH levels. Each component of glutathione antioxidants contributes to the intracellular antioxidant capacity, which maintains the cellular redox status [37]. The biphasic or even triphasic responses are likely related to the redox-sensitive feedback mechanism, which can be fine-tuned in response to the changes in cellular redox status caused by the pro-oxidant effect of (−)Sch B. While GCLm is responsible for regulating the rate of *de novo* synthesis of GSH, GR and G6DPH directly or indirectly control the cellular glutathione redox cycling, and both processes are critical for the recovery of GSH after oxidant challenge [38]. The increased expression of these enzymes is instrumental in rescuing cells from oxidant-induced apoptosis, which can cause acute glutathione depletion and the subsequent execution of apoptosis [39]. A recent study has demonstrated that the cellular capacity of GR-catalysed GSH recovery rather than the GSH level is a determinant factor for cell survival under conditions of oxidative stress [40].

Our results showed that menadione challenge differentially activated all three MAPK. Presumably, ROS generated during menadione intoxication activated the MAPK, as was the case for CYP-catalysed reaction with (−)Sch B in AML12 cells. (−)Sch B treatment was found to potentiate menadione-induced ERK activation, but both p38 and JNK activations were

attenuated in (−)Sch B-pre-treated cells. While superoxide anions arising from the intracellular metabolism of menadione were found to trigger the JNK signalling pathway and the associated apoptosis, the activation of ERK signalling cascade attenuated the apoptosis [41]. Furthermore, a prolonged and robust JNK activation has been shown to be apoptotic [39]. Nevertheless, the beneficial effect of (−)Sch B-induced potentiation of ERK activation and suppression of JNK/p38 activation in menadione-intoxicated cells was supported by a reduced AIF release during the course of menadione challenge, with a resultant inhibition of apoptotic cell death. It has been shown that the release of AIF from mitochondria plays an important role in caspase-independent programmed cell death [42]. The determining role of ERK/Nrf2 signalling in the hepatoprotection afforded by Sch B was confirmed by the finding that Sch B pre-treatment did not confer a hepatoprotective effect under the condition of ERK inhibition in mice and this observation was correlated well with the suppression of the Sch B-induced glutathione antioxidant response as assessed by mitochondrial GSH level.

In conclusion, several lines of evidence from our studies indicate that (−)Sch B triggers a redox-sensitive ERK/Nrf2 signalling, which then elicits a cellular glutathione antioxidant response and protects against menadione-induced apoptosis in AML12 hepatocytes. The ERK-mediated signalling is also involved in the Sch B-induced hepatoprotection against CCl_4 hepatotoxicity in mice.

Declaration of interest

This work was supported by a GRF Grant (Project Number: 661107) (Principal Investigator Dr K. M. Ko) from the Research Grants Council, Hong Kong.

The authors report no conflicts of interest. The authors alone are responsible for the content and writing of the paper.

References

[1] Ko RKM, Mak DHF. Schisandrin B and other Dibenzocyclooctadiene lignans. In: Packer L, Halliwell B, Ong CN, editors. Herbal and traditional medicine: molecular aspects of health. New York, Basel, Hong Kong: Marcel Dekker; 2004. p 289–314.

[2] Ip SP, Poon MK, Wu SS, Che CT, Ng KH, Kong YC, Ko KM. Effect of schisandrin B on hepatic glutathione antioxidant system in mice: protection against carbon tetrachloride toxicity. Planta Medica 1995;61:398–401.

[3] Chiu PY, Tang MH, Mak DHF, Poon MTK, Ko KM. Hepatoprotective mechanism of schisandrin B: role of mitochondrial glutathione antioxidant status and heat shock proteins. Free Radic Biol Med 2003;35:368–380.

[4] Chiu PY, Mak DHF, Poon MTK, Ko KM. Role of cytochrome P-450 in schisandrin B-induced antioxidant and heat shock responses in mouse liver. Life Sci 2005;77:2887–2895.

[5] Chiu PY, Leung HY, Poon MTK, Lee SST, Ko KM. Schisandrin B induced antioxidant response is partly mediated by cytochrome P-4502E1 catalyzed reaction in mouse liver. Mol Cell Biol 2006;293:87–92.

[6] Chiu PY, Leung HY, Siu AHL, Poon MTK, Ko KM. Schisandrin B decreases the sensitivity of mitochondria to calcium ion-induced permeability transition and protects against carbon tetrachloride toxicity in mouse livers. Biol Pharm Bull 2007;30:1108–1112.

[7] Chiu PY, Ko KM. Schisandrin B-induced increase in cellular glutathione level and protevtion against oxidant injury are mediated by the enhancement of glutathione synthesis and regeneration in AML12 and H9c2 cells. Biofactors 2006;26:221–230.

[8] Chiu PY, Leung HY, Poon MTK, Mak DHF, Ko KM. Effects of schisandrin B enantiomers on cellular glutathione and menadione toxicity in AML12 hepatocytes. Pharmacology 2006;77:63–70.

[9] Chiu PY, Luk KF, Leung HY, Ng KM, Ko KM. Schisandrin B stereoisomers protect against hypoxia/reoxygenation-induced apoptosis and associated changes in the calcium ion-induced mitochondrial permeability transition and mitochondrial membrane potential in AML12 hepatoctes. Phytotherapy Res 2009;23:1592–1602.

[10] Baek MS, Kim JY, Myung SW, Yim YH, Jeong JH, Kim DH. Metabolism of dimethyl-4,4'-dimethoxy-5,6,5',6'-dimethylene dioxybiphenyl-2,2'-dicarboxylate (DDB) by human liver microsomes: characterization of metabolic pathways and of cytochrome P450 isoforms involved. Drug Metab Dispos 2001;29:381–388.

[11] Leong PK, Chiu PY, Leung HY, Ko KM. Cytochrome P-450-catalyzed reactive oxygen species production mediates the (−)Schisandrin B-induced glutathione and heat shock responses in AML12 hepatocytes. Cell Biol Int 2010; In press.

[12] D'Autreaux B, Toledano MB. ROS as signalling molecules: mechanisms that generate specificity in ROS homeostasis. Nat Rev Mol Cell Biol 2007;8:813–824.

[13] McCubrey JA, Lahair MM, Franklin RA. Reactive oxygen species-induced activation of the MAP kinase signaling pathways. Antioxid Redox Signal 2006;8:1775–1789.

[14] Torres M, Forman HJ. Redox signaling and the MAP kinase pathways. Biofactors 2003;17:287–296.

[15] Johnson GL, Lapadat R. Mitogen-activated protein kinase pathways mediated by ERK, JNK, and p38 protein kinases. Science 2002;298:1911–1912.

[16] Dougherty CJ, Kubasiak LA, Prentice H, Andreka P, Bishopric NH, Webster KA. Activation of c-Jun N-terminal kinase promotes survival of cardiac myocytes after oxidative stress. Biochem J 2002;362:561–571.

[17] Tanos T, Marinissen MJ, Leskow FC, Hochbaum D, Martinetto H, Gutkind JS, Coso OA. Phosphorylation of c-Fos by members of the p38 MAPK family. Role in the AP-1 response to UV light. J Biol Chem 2005;280:18842–18852.

[18] Crowe DL, Shemirani B. The transcription factor ATF-2 inhibits extracellular signal regulated kinase expression and proliferation of human cancer cells. Anticancer Res 2000;20:2945–2949.

[19] Echave P, Machado-da-Silva G, Arkell RS, Duchen MR, Jacobson J, Mitter R, Lloyd AC. Extracellular growth factors and mitogens cooperate to drive mitochondrial biogenesis. J Cell Sci 2009;122:4516–4525.

[20] Xu C, Yuan X, Pan Z, Shen G, Kim JH, Yu S, Khor TO, Li W, Ma J, Kong AN. Mechanism of action of isothiocyanates: the induction of ARE-regulated genes is associated with activation of ERK and JNK and the phosphorylation and nuclear translocation of Nrf2. Mol Cancer Ther 2006;5:1918–1926.

[21] Huang HC, Nguyen T, Pickett CB. Phosphorylation of Nrf2 at Ser-40 by protein kinase C regulates antioxidant response element-mediated transcription. J Biol Chem 2002;277:42769–42774.

[22] Copple IM, Goldring CE, Kitteringham NR, Park BK. The Nrf2-Keap1 defence pathway: role in protection against drug-induced toxicity. Toxicology 2008;246:24–33.
[23] Jeyapaul J, Jaiswal AK. Nrf2 and c-Jun regulation of antioxidant response element (ARE)-mediated expression and induction of gamma-glutamylcysteine synthetase heavy subunit gene. Biochem Pharmacol 2000;59:1433–1439.
[24] Liu XP, Goldring CE, Copple IM, Wang HY, Wei W, Kitteringham NR, Park BK. Extract of Ginkgo biloba induces phase 2 genes through Keap1-Nrf2-ARE signaling pathway. Life Sci 2007;80:1586–1591.
[25] Griffith OW. Determination of glutathione and glutathione disulfide using glutathione reductase and 2-vinylpyridine. Anal Biochem 1980;106:207–212.
[26] Cullinan SB, Zhang D, Hannink M, Arvisais E, Kaufman RJ, Diehl JA. Nrf2 is a direct PERK substrate and effector of PERK-dependent cell survival. Mol Cell Biol 2003;23: 7198–7209.
[27] Erfle H, Neumann B, Rogers P, Bulkescher J, Ellenberg J, Pepperkok R. Work flow for multiplexing siRNA assays by solid-phase reverse transfection in multiwell plates. J Biomol Screen 2008;13:575–580.
[28] Chang F, Steelman LS, Shelton JG, Lee JT, Navolanic PM, Blalock WL, Franklin R, McCubrey JA. Regulation of cell cycle progression and apoptosis by the Ras/Raf/MEK/ERK pathway (Review). Int J Oncol 2003;22:469–480.
[29] Tobiume K, Matsuzawa A, Takahashi T, Nishitoh H, Morita K, Takeda K, Minowa O, Miyazono K, Noda T, Ichijo H. ASK1 is required for sustained activations of JNK/p38 MAP kinases and apoptosis. EMBO Rep 2001;2:222–228.
[30] Yuan X, Xu C, Pan Z, Keum YS, Kim JH, Shen G, Yu S, Oo KT, Ma J, Kong AN. Butylated hydroxyanisole regulates ARE-mediated gene expression via Nrf2 coupled with ERK and JNK signaling pathway in HepG2 cells. Mol Carcinog 2006; 45:841–850.
[31] Na HK, Kim EH, Jung JH, Lee HH, Hyun JW, Surh YJ. (-)-Epigallocatechin gallate induces Nrf2-mediated antioxidant enzyme expression via activation of PI3K and ERK in human mammary epithelial cells. Arch Biochem Biophys 2008;476: 171–177.

This paper was first published online on Early Online on 28 January 2011.

[32] Ardanaz N, Pagano PJ. Hydrogen peroxide as a paracrine vascular mediator: regulation and signaling leading to dysfunction. Exp Biol Med 2006;231:237–251.
[33] Ushio-Fukai M, Alexander RW, Akers M, Griendling KK. p38 Mitogen-activated protein kinase is a critical component of the redox-sensitive signaling pathways activated by angiotensin II. Role in vascular smooth muscle cell hypertrophy. J Biol Chem 1998;273:15022–15029.
[34] Nguyen T, Nioi P, Pickett CB. The Nrf2-antioxidant response element signaling pathway and its activation by oxidative stress. J Biol Chem 2009;284:13291–13295.
[35] Chen M, Gu H, Ye Y, Lin B, Sun L, Deng W, Zhang J, Liu J. Protective effects of hesperidin against oxidative stress of tert-butyl hydroperoxide in human hepatocytes. Food Chem Toxicol 2010;48:2980–2987.
[36] Sun Z, Huang Z, Zhang DD. Phosphorylation of Nrf2 at multiple sites by MAP kinases has a limited contribution in modulating the Nrf2-dependent antioxidant response. PLoS One 2009;4:e6588.
[37] Zhang Q, Pi J, Woods CG, Andersen ME. A systems biology perspective on Nrf2-mediated antioxidant response. Toxicol Appl Pharmacol 2010;244:84–97.
[38] Han D, Hanawa N, Saberi B, Kaplowitz N. Mechanisms of liver injury. III. Role of glutathione redox status in liver injury. Am J Physiol Gastrointest Liver Physiol 2006;291:G1–G7.
[39] Circu ML, Aw TY. Reactive oxygen species, cellular redox systems, and apoptosis. Free Radic Biol Med 2010;48:749–762.
[40] Harvey CJ, Thimmulappa RK, Singh A, Blake DJ, Ling G, Wakabayashi N, Fujii J, Myers A, Biswal S. Nrf2-regulated glutathione recycling independent of biosynthesis is critical for cell survival during oxidative stress. Free Radic Biol Med 2009;46:443–453.
[41] Conde de la Rosa L, Schoemaker MH, Vrenkenm TE, Buist-Homan M, Havinga R, Jansen PL, Moshage H. Superoxide anions and hydrogen peroxide induce hegical roles of ASK1-MAP kinase pathway in stress signaling. Biochim Biophys Acta 2008;1780:1325–1336.
[42] Lorenzo HK, Susin SA. Therapeutic potential of AIF-mediated caspase-independent programmed cell death. Drug Res Updates 2007;10:235–255.